ELSEVIER

Coordination Chemistry Reviews 231 (2002) 83–108

COORDINATION CHEMISTRY REVIEWS

www.elsevier.com/locate/ccr

Metal carbonyl cations: generation, characterization and catalytic application

Qiang Xu *

National Institute of Advanced Industrial Science and Technology (AIST), 1-8-1 Midorigaoka, Ikeda, Osaka 563-8577, Japan

Received 2 November 2001; received in revised form 6 February 2002

Contents

Abstract

There has been a rapid development in the study of metal carbonyl cations, which exhibit distinguishing characteristics in comparison with typical metal carbonyl complexes. This review article gives an overview of the generation, spectroscopic characterization and catalytic application of this new class of metal carbonyls, including the metal carbonyl cluster cations. © 2002 Elsevier Science B.V. All rights reserved.

Keywords: Metal carbonyls; Cations; Clusters; Synthesis; Spectroscopy; Catalysts

1. Introduction

Carbon monoxide is one of the most important and versatile ligands in transition metal chemistry [1]. Since the discovery of the first metal carbonyl complexes,

* Fax: +81-727-51-9629
E-mail address: q.xu@aist.go.jp (Q. Xu).

PII: S0010-8545(02)00115-7

$Pt(CO)_2Cl_2$, $Pt_2(CO)_4Cl_4$, and $Pt_2(CO)_3Cl_4$, by Schützenberger in 1868 [2–5], and the discovery of the first homoleptic metal carbonyl, $Ni(CO)_4$, by Mond in 1890 and its immediate industrial application for the preparation of ultrapure nickel [6–8], metal carbonyls have played a very important role in chemistry and the chemical industry [9,10]. Many industrial processes employ CO as a reagent and transition metal compounds as heterogeneous or homogeneous catalysts and involve the intermediates of metal carbonyls [11–15].

Carbon monoxide can bind in a terminal or multiply bridging fashion to a host of charged and uncharged metal atoms, clusters, organometallic fragments, and surfaces of metals or ionic crystals and give products ranging from diverse molecular complexes, through adsorbates, to matrix-isolated molecules. The metal–carbonyl bonding is suggested to involve a synergistic interaction between σ-donor bonding from the occupied 5σ molecular orbital of CO into an empty metal orbital with σ symmetry and π-backbonding from occupied metal orbitals into the π* molecular orbitals of CO [1].

Recently, there have been remarkable developments in the more than 100 years-old chemistry of metal carbonyls [16,17]. A number of highly-reduced metal carbonyl anions (carbonylmetalates) containing metals in negative formal oxidation states have been obtained through chemical reduction in basic solvents [18–20]. An increasing number of new homoleptic metal carbonyl cations and their derivatives, in which the CO ligand primarily functions as a σ donor, have been prepared in acidic or superacidic media or with weakly coordinating anions [21–28]. In addition, our knowledge of relatively stable neutral carbonyl complexes has also been remarkably enriched and the expectation of further developments in metal carbonyl chemistry have been made by the synthesis of the first metalloidal and alkaline earth metal carbonyls, $[Cp^*_2Si(CO)](Cp^* = C_5Me_5)$ [29] and $[Cp^*_2Ca(CO)]$ [30], respectively, in solution and by the isolation and X-ray structural characterization of the first f-block metal carbonyl complex, $[(C_5Me_4H)_3U(CO)]$ [31,32], all of which include the important ligand pentamethylcyclopentadienyl or its derivatives [33,34].

In this review, we focus on the generation, spectroscopic characterization and catalytic application of the homoleptic carbonyl cations and cationic carbonyl derivatives of metals from Groups 6 through 12 in formal oxidation states ranging from +1 to +6, which are characterized by high CO stretching frequencies, ν(CO). Related cationic metal carbonyl species isolated in rare-gas matrices, CO adducts to metal oxides and halides and metal-exchanged zeolites will be described. Much attention will be paid to the new homoleptic metal carbonyl cluster cations, of which the number is still limited to three but expected to increase. The discussion will also include the metal hydridocarbonyl (cluster) cations formed by the protonation of neutral metal carbonyl (cluster) complexes with the metal atoms kept in the formal oxidation state 0, which exhibit properties related to the metal carbonyl (cluster) cations in which the metal atoms are in the formal oxidation states $\geq +1$.

2. Generation and characterization of metal carbonyl cations

2.1. Mononuclear metal carbonyl cations and related species

2.1.1. Historical perspective

It is indeed interesting that *cis*-$Pt(CO)_2Cl_2$, the first metal carbonyl discovered 130 years ago [2–5], is now, because of its high ν(CO) ($\nu(CO)_{av} = 2165\ cm^{-1}$) [35–39], considered to be a member of the new class of metal carbonyls, in which the CO ligand functions primarily as a σ donor. This new class, i.e. the metal carbonyl cations and their cationic derivatives, remains a small group (~ 1%) in the metal carbonyl family, but is increasing in number and importance.

Historically, Manchot and co-workers are the first to systematically investigate the metal carbonyl compounds that were later shown to be primarily σ-bonded. During the beginning of the last century, they repeated the synthesis of the platinum carbonyl chlorides first described by Schützenberger [40]. In addition they discovered the first carbonyl derivative of palladium with the composition $Pd(CO)Cl_2$ [41], and the first carbonyl derivative of gold, Au(CO)Cl [42]. The first use was made by them of a strong protic acid (concentrated H_2SO_4) in the attempted preparation of silver carbonyl cations [43,44], which is the prototype for the recent syntheses of metal carbonyl cations. Most of the above noble metal carbonyl species are now considered to be primarily σ-bonded.

In the 1950–1960s, there appeared examples of cationic transition metal carbonyl species exhibiting ν(CO) values higher than 2143 cm^{-1}, the value for free CO. They involve, for example, $Cu(CF_3CO_2)(CO)$ (2155 cm^{-1}) [45], $[Pt(CO)Cl_2]_2$ (2152 cm^{-1}) [46,47], $[Fe(CO)_5Cl]BCl_4$ (2210 cm^{-1}) [48], $[Fe(CO)_5Br]BCl_4$ (2200 cm^{-1}) [48], $[Fe(CO)_5NO]Cl$ (2200 cm^{-1}) [48] and $[Fe(CO)_5H]PF_6$ (2196 cm^{-1}) [48]; the high ν(CO) values were suggested to arise from the reduced amount of π-backbonding [47,49]. High ν(CO) frequencies close to 2200 cm^{-1} were also observed for CO adsorbed on the surfaces of metal oxides such as NiO [50,51] or in a series of alkali, alkaline earth and transition metal-exchanged zeolites [52], for which the polarization of the carbon monoxide molecule in the electric field was suggested to be responsible.

The first thermally stable homoleptic carbonyl cations, octahedral $[M(CO)_6]^+$ (M = Mn, Tc, Re), were isolated by Fischer, Hieber and their co-workers in 1961 [53–57]. About 30 years then passed before the isolation of the next homoleptic metal carbonyl cation, $[Au(CO)_2]^+$; its discovery resulted as an accident from the attempts to prepare the $[HCO]^+$ ion by protonation of CO in the conjugated superacid HSO_3F–$Au(SO_3F)_3$ and its isolation required the development of a new carbonylation method in Lewis superacidic media such as SbF_5 [58,59]. In SbF_5, a number of thermally stable salts of metal carbonyl cations have subsequently been isolated and characterized spectroscopically and structurally [24,28]. Several homoleptic metal carbonyl cations have been isolated using weakly coordinating anions such as $[B(OTeF_5)_4]^-$ [60–62] and $[1\text{-Et-}CB_{11}F_{11}]^-$ [63,64] in organic solvents. In the meantime, a number of metal carbonyl cations have been generated in protic acids, which are used for spectroscopic characterization and applied as catalysts for the carbonylation of olefins and other organic compounds [25,65–71]. In addition, related cationic metal carbonyl species have been formed in zeolites and on the surfaces of metal oxides and halides [72], and a new laser-ablation technique has recently been successfully employed to isolate a series of metal carbonyl cations in rare-gas matrices which have been characterized in detail by FTIR [73].

2.1.2. Isolable and soluble metal carbonyl cations and cationic carbonyl derivatives

Most of the homoleptic neutral metal carbonyls reported so far are obtained from metal halogenides or oxides at high temperature and high CO pressure in the presence of reducing agents such as CO, H_2, and alkali metals [1]. Only $Ni(CO)_4$ and $Fe(CO)_5$ can be directly obtained from the metals [6,74,75]. The simplest and most straightforward approach to metal carbonyl anions (carbonylmetalates) is via the reduction of neutral metal carbonyls, usually with alkali metals, whereby a CO–ligand (two-electron donor) is formally replaced by two electrons or a metal–metal bond is reductively cleaved [19,20]. Another route to carbonylmetalates is the direct reduction of metal halogenides by alkali metals in basic solvents [19,20].

In contrast to the preparation methods for neutral and anionic metal carbonyl complexes, the metal carbonyl cations and the cationic derivatives, owing to their high electrophilicity, are usually synthesized in acidic or superacidic media. The pioneering synthesis of $[M(CO)_6]^+$ (M = Mn, Tc, Re) by Fischer, Hieber and their co-workers includes halide abstraction from $M(CO)_5X$ (X = Cl, Br) with Lewis acids like $M'X_3$ (M′ = Al, Fe; X = Cl, Br) at high temperature and CO pressure [53–57]. Using the same method, the compounds $[Ir(CO)_4][AlCl_4]$ [76] and $[Rh(CO)_4][Al_2Cl_7]$ [77,78] have recently been isolated from $Ir(CO)_3Cl$ and $[Rh(CO)_2Cl]_2$, respectively.

$$M(CO)_5X + AlCl_3 + CO \xrightarrow[200\ atm\ CO]{100\ ^\circ C} [M(CO)_6][AlCl_3X] \quad (M = Mn,\ Tc,\ Re)$$

$$Ir(CO)_3Cl + CO + AlCl_3 \xrightarrow{150\ ^\circ C} [Ir(CO)_4][AlCl_4]$$

Below are described the respective approaches to the metal carbonyl cations (Table 1). There are, interestingly, several examples of the same metal carbonyl cation being prepared in different ways.

2.1.2.1. In Lewis superacid SbF_5. Willner, Aubke and co-workers have isolated a series of metal carbonyl cations with the counteranion $[Sb_2F_{11}]^-$ in the Lewis superacid SbF_5 [24]. All of the thermally stable $[Sb_2F_{11}]^-$ salts of the metal carbonyl cations can be prepared by one of the following three synthetic methods: (a) solvolysis and carbonylation, (b) reductive carbonylation, and (c) oxidative carbonylation.

The synthetic method of solvolysis and carbonylation was first employed to isolate the linear $[Au(CO)_2]^+$ [59]. Attempts to isolate $[Au(CO)_2]^+$ by removing the solvent HSO_3F and the volatile reaction products in vacuo were unsuccessful, leading only to the carbonyl gold(I) sulfate, $Au(CO)SO_3F$, since SO_3F^- is sufficiently basic to compete with CO for a coordination site on gold [58]. The solvolysis of $Au(CO)SO_3F$ in SbF_5 in the presence of CO results in the formation of the thermally stable $[Au(CO)_2][Sb_2F_{11}]$ salt [59]. This method has been successfully employed for isolating the linear $[Hg(CO)_2]^{2+}$ from $Hg(SO_3F)_2$ [109,110], the octahedral $[M(CO)_6]^+$ (M = Mn, Re) from $M(CO)_5Cl$ [99], and the square-planar $[M(CO)_4]^{2+}$ (M = Pd, Pt) from MCl_2 [99]. During the solvolysis, the oxidation state of the metal in the starting compound remains unchanged.

$$Au(SO_3F)_3 + 3CO \xrightarrow[25\ ^\circ C]{HSO_3F} [Au(CO)_2]^+ + CO_2 + S_2O_5F_2 + SO_3F^-$$

$$[Au(CO)_2]^+ + SO_3F^- \xrightarrow[80\ ^\circ C]{HSO_3F} Au(CO)SO_3F + CO$$

$$Au(CO)SO_3F + CO + 4SbF_5 \xrightarrow{SbF_5} [Au(CO)_2][Sb_2F_{11}] + Sb_2F_9SO_3F$$

In reductive carbonylation, solvolysis is accompanied by reduction of the metal salt with CO acting as a reducing agent and ligand. Using this method, the square-planar $[Pt(CO)_4]^{2+}$ and $[Pd(CO)_4]^{2+}$ [77], the octahedral $[M(CO)_6]^{2+}$ (M = Ru, Os) [89] and the octahedral $[Ir(CO)_6]^{3+}$ [92], in which the +3 oxidation state of Ir is the highest of all the homoleptic metal carbonyl cations known, have been isolated from $Pt(SO_3F)_4$, $Pd(SO_3F)_3$, $M(SO_3F)_3$ (M = Ru, Os) and IrF_6, respectively, in SbF_5. The novel complex *trans*-

Table 1
Vibrational, ^{13}C-NMR and structural data of homoleptic metal carbonyl cations and related carbonyl derivatives

Compound	ν(CO)$_{IR}$ (cm^{-1})	ν(CO)$_{Raman}$ (cm^{-1})	δ(^{13}C) (ppm)	d(MC) (Å)	d(CO) (Å)	References
$[\{Mo(CO)_4\}_2(cis\text{-}\mu\text{-}F_2SbF_4)_3]^+$ [a]	2156, 2105, 2092, 2086	2156, 2105, 2088, 2085		2.021–2.052	1.089–1.136	[79]
$[W(CO)_6(FSbF_5)]^+$ [a]	2205, 2170, 2147, 2088, 2075, 2064	2206, 2170, 2146, 2084, 2078, 2060		1.996–2.150	1.109–1.160	[80]
$[Mn(CO)_6]^+$ [a]	2100	2185, 2128	195			[24,81]
$[Re(CO)_6]^+$ [a]	2085	2197, 2122	171	1.89–2.07 [b]	1.12–1.19 [b]	[24,82–86]
$[Fe(CO)_6]^{2+}$ [a]	2204	2241, 2220	178	1.911	1.104	[87,88]
$[Ru(CO)_6]^{2+}$ [a]	2199	2254, 2222	166			[89]
trans-$[OsO_2(CO)_4]^{2+}$ [a]	2253	2280, 2269	134			[90]
$[Os(CO)_6]^{2+}$ [a]	2190	2259, 2218	147			[89]
$Co(CO)_4(L)^+$ [c]	2155, 2139, 2122	2195, 2156, 2141, 2128	186			[68]
$[Rh(CO)_5Cl]^{2+}$ [a]	2273, 2240	2272, 2240		1.999–2.032	1.087–1.107	[91]
$[Rh(CO)_4]^+$ [d]	2138	2215, 2176	172 [e]	1.947–1.958	1.109–1.124	[63,67,68,77]
$[Ir(CO)_6]^{3+}$ [a]	2254	2295, 2276	121			[92]
$[Ir(CO)_5Cl]^{2+}$ [a]	2279, 2227	2279, 2228		2.00–2.05	1.07–1.12	[91,92]
mer-$Ir(CO)_3(SO_3F)_3$	2249, 2208, 2198	2249, 2206, 2196		1.937–2.006	1.094–1.114	[93]
fac-$Ir(CO)_3F_3$ [f]	2213, 2165		131	2.03 [g]		[94,95]
$[Ir(CO)_4]^+$ [h]	2125	2216, 2170				[76]
$[Pd(CO)_4]^{2+}$ [a]	2249	2278, 2263	144	1.984–2.006	1.100–1.111	[77,96]
cis-$Pd(CO)_2(SO_3F)_2$	2228, 2208	2228, 2207	145	1.919, 1.945	1.102, 1.114	[24,97,98]
$[c\text{-}Pd_2(\mu\text{-}CO)_2]^{2+}$ [a]	2006	2048				[99]
$[c\text{-}Pd_2(\mu\text{-}CO)_2](SO_3F)_2$	1977	2027	162 [e]	1.966, 1.984	1.133	[24,100]
$[Pt(CO)_4]^{2+}$ [a]	2244	2289, 2267	137	1.979–1.987	1.086–1.118	[77,96,101]
cis-$Pt(CO)_2(SO_3F)_2$	2219, 2185	2218, 2181	131	1.868, 1.897	1.103, 1.130	[24,39,97]
$[(dfepe)Pt(CO)_2]^{2+}$ [e]	2235, 2222		153 [i]			[102]
cis-$Pt(CO)_2Cl_2$	2190, 2152	2189, 2146	152 [j]	1.893, 1.901	1.121, 1.110	[37–39]
$[\{Pt(CO)_3\}_2]^{2+}$ [k]	2218, 2187, 2174	2233, 2209, 2219, 2194, 2173	166, 159	1.960 [g]		[69,70]
$[Cu(CO)_4]^+$ [d]	2184	2181 [e]	171 [e]	1.961–1.968	1.109–1.114	[64,103,104]
$Cu(CO)_2(N(SO_2CF_3)_2)$	2184, 2158			1.895, 1.906	1.130, 1.115	[105]
$[Ag(CO)_2]^+$	2196 [l]	2220 [l]	172 [m]	2.06–2.20 [n]	1.07–1.09 [n]	[61,62]
$[Ag(CO)]^+$	2204 [l]	2206 [l]	171 [m]	2.10 [n]	1.077 [n]	[60,62]
$[Au(CO)_2]^{2+}$ [a]	2217	2254	174 [e]	1.962–1.982 [o]	1.107–1.153 [o]	[59,106]
$Au(CO)SO_3F$	2195	2198	162 [e]			[58,59]
Au(CO)Cl	2162 [j]	2183	172 [j]	1.93	1.11	[35,107,108]
$[Hg(CO)_2]^{2+}$ [a]	2278	2281	169	2.083	1.104	[109,110]
$[\{Hg(CO)_2\}_2]^{2+}$ [a]	2247	2248	189			[109,110]
$W(CO)_6$	1977	2115, 1998	192	2.058 [p]	1.148 [p]	[111–113]
CO [q]	2143		184		1.128	[59,108,114,115]
$CO^+(X^2\Sigma^+)$ [q]	2184				1.115	[115]
$[HCO]^+$ [q]	2184		140 [r]		1.107	[116–118]

[a] As salt of $[Sb_2F_{11}]^-$.
[b] As salt of $[Re_2F_{11}]^-$.
[c] In $HSO_3F \cdot SbF_5$ (1:1).
[d] As salt of $[1\text{-}Et\text{-}CB_{11}F_{11}]^-$.
[e] In HSO_3F.
[f] In HF solution.
[g] EXAFS data.
[h] As salt of $[AlCl_4]^-$.
[i] In SbF_5.
[j] In CH_2Cl_2.
[k] In concentrated H_2SO_4.
[l] As salt of $[Nb(OTeF_5)_6]^-$.
[m] As salt of $[Zn(OTeF_5)_4]^{2-}$.
[n] As salt of $[B(OTeF_5)_4]^-$.
[o] As salt of $[SbF_6]^- \cdot [Sb_2F_{11}]^-$.
[p] Electron diffraction data.
[q] Gas phase.
[r] In $HF \cdot SbF_5$ (1:1).

$[OsO_2(CO)_4]^{2+}$, in which the +6 oxidation state of Os is the highest in all the metal carbonyl cations known, is formed from OsO_4 in SbF_5 [90]. The alternative simplified synthetic route to $[Au(CO)_2][Sb_2F_{11}]$ is the direct reductive carbonylation of $Au(SO_3F)_3$ or $AuCl_3$ in SbF_5 [99].

$$2M(SO_3F)_3 + 16SbF_5 + 13CO \xrightarrow[1\ atm\ CO,\ 60\text{–}90\ ^\circ C]{SbF_5} 2[M(CO)_6][Sb_2F_{11}]_2 + CO_2 + S_2O_5F_2 + 4Sb_2F_9(SO_3F)$$

(M = Ru or Os)

$$Au(SO_3F)_3 + 3CO + 4SbF_5 \xrightarrow[1\ atm\ CO,\ 65\ ^\circ C]{SbF_5} [Au(CO)_2][Sb_2F_{11}] + CO_2 + S_2O_5F_2 + Sb_2F_9(SO_3F)$$

Two types of oxidative carbonylations have been reported for preparing metal carbonyl cations from neutral metal carbonyl derivatives. As the first type, the octahedral $[Fe(CO)_6]^{2+}$ has been isolated from SbF_5 with different external oxidizing agents of Cl_2, AsF_5, and XeF_2, respectively [87,88]. As the second type, SbF_5 serves simultaneously as an oxidizing agent and reaction medium in the transformation of $Mn_2(CO)_{10}$, $W(CO)_6$, $Mo(CO)_6$, $[Rh(CO)_2Cl]_2$ and $[Ir(CO)_3Cl]$ with CO into $[Mn(CO)_6][Sb_2F_{11}]$ [24], $[W(CO)_6(FSbF_5)][Sb_2F_{11}]$ [80], $[\{Mo(CO)_4\}_2(cis\text{-}\mu\text{-}F_2SbF_4)_3]_x[Sb_2F_{11}]_x$ [79], $[Rh(CO)_5Cl][Sb_2F_{11}]_2$ [91] and $[Ir(CO)_5Cl][Sb_2F_{11}]_2$ [91], respectively.

$$Fe(CO)_5 + XeF_2 + CO + 4SbF_5 \xrightarrow[50\ ^\circ C,\ 1\ atm\ CO]{HF\text{–}SbF_5} [Fe(CO)_6][Sb_2F_{11}]_2 + Xe$$

$$6W(CO)_6 + 29SbF_5 \xrightarrow[40\ ^\circ C,\ 2\ atm\ CO]{HF\text{–}SbF_5} 6[W(CO)_6(FSbF_5)][Sb_2F_{11}] + 6SbF_3 \cdot 5SbF_5$$

2.1.2.2. CO addition to metal salts with weakly coordinating anions. Another route to metal carbonyl cations is the reversible CO addition to coordinatively unsaturated metal salts with bulky weakly coordinating anions [119] under a CO atmosphere. Strauss and co-workers have isolated the $[Ag(CO)]^+$ and $[Ag(CO)_2]^+$ cations by the direct but reversible CO addition to the silver(I) salts of $[B(OTeF_5)_4]^-$, $[Zn(OTeF_5)_4]^{2-}$, $[Nb(OTeF_5)_6]^-$, and $[Ti(OTeF_5)_6]^{2-}$ under different CO pressures; single-crystals of $[Ag(CO)][B(OTeF_5)_4]$ and $[Ag(CO)_2][B(OTeF_5)_4]$ were obtained from the very weakly coordinating solvent 1,1,2-$C_2Cl_3F_3$, and their low temperature X-ray diffraction studies revealed nearly linear Ag–C–O arrays in both of the salts and a linear structure for $[Ag(CO)_2][B(OTeF_5)_4]$ [60–62]. The direct but reversible CO addition to metal salts with weakly coordinating anions results in the formation of $[Cu(CO)_n][AsF_6]$ ($n = 1, 2, 3$) [120], $[Ag(CO)_3][Nb(OTeF_5)_6]$ [121] and $[Ag(CO)_n][B(CF_3)_4]$ ($n = 1$–4) [122]. The exposure of $[Au(CO)_2][Sb_2F_{11}]$ to CO at a pressure as high as 100 atm leads to the reversible formation of $[Au(CO)_3][Sb_2F_{11}]$ [123].

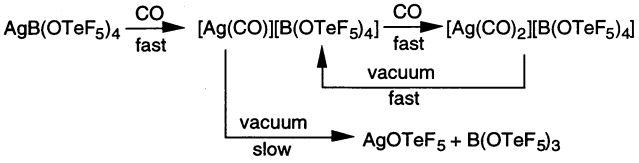

Another weakly coordinating anion $[1\text{-Et-}CB_{11}F_{11}]^-$ has been used to prepare the tetrahedral $[Cu(CO)_4]^+$ [64] and square-planar $[Rh(CO)_4]^+$ [63] cations; the synthesis involves the metathesis reaction of Ag[1-Et-$CB_{11}F_{11}$] with CuCl or $[Rh(CO)_2Cl]_2$ and subsequent CO addition under a CO atmosphere. Furthermore, $Cu(CO)_2(N(SO_2CF_3)_2)$ is formed by treating a CH_2Cl_2 solution of mesitylcopper(I) and $HN(SO_2CF_3)_2$ with 1.3 atm of CO at 0 °C; placing this complex under vacuum or at high pressure results in the formation of $Cu(CO)(N(SO_2CF_3)_2)$ or $Cu(CO)_3(N(SO_2CF_3)_2)$ [105]. As a related example, the metathesis followed by CO addition with the appropriate metal complexes has been used to prepare the $[HB(3,5\text{-}(CF_3)_2Pz)_3]M(CO)$ (M = Cu, Ag, Au) complexes [124–126].

$$[Rh(CO)_2Cl]_2 + 2Ag[1\text{-Et-}CB_{11}F_{11}] + 4CO \xrightarrow[-2AgCl]{CH_2Cl_2} 2[Rh(CO)_4][1\text{-Et-}CB_{11}F_{11}]$$

2.1.2.3. In protic acids. Protic acids have been used to generate a number of metal carbonyl cations and cationic carbonyl derivatives as well as molecular adducts of CO to metal cations, as first done by Manchot and co-workers in 1920s [43,44]. The reactions can also be divided to three types: (a) solvolysis and carbonylation, (b) reductive carbonylation, and (c) oxidative carbonylation. The two protic superacids HSO_3F and anhydrous hydrogen fluoride HF are very suited for the preparation of metal carbonyl fluorosulfates and fluorides, which include $Au(CO)SO_3F$ [58], *cis*-$Pd(CO)_2(SO_3F)_2$ [97,98], *cis*-$Pt(CO)_2(SO_3F)_2$ [39,97], *mer*-$Ir(CO)_3(SO_3F)_3$ [93], [*cyclo*-$Pd_2(\mu\text{-}CO)_2](SO_3F)_2$ [100] and *fac*-$Ir(CO)_3F_3$ [94,95]. In particular, a number of solvated cationic metal carbonyl complexes (for sake of brevity, solvated cations that should exist in the form of $[M(CO)_n(L)_m]^{a+}$ (L denotes the weakly coordinating ligand probably being the conjugate base of the solvent acid or a closely related species) will be simply formulated as $M(CO)_n^{a+}$), including $Cu(CO)_n^+$ ($n = 1$–4) [103,127], $Ag(CO)_n^+$ ($n = 1$–3) [103,127], $Au(CO)_n^+$ ($n = 1, 2$) [58,65], $Co(CO)_4^+$ [68], $[Rh(CO)_4]^+$ [67,68], $[Pt(CO)_4]^{2+}$ [101], [*cyclo*-$Pd_2(\mu\text{-}CO)_2]^{2+}$ [66] and $[\{Pt(CO)_3\}_2]^{2+}$ [69–71], are formed in protic acids, most of which exhibit catalytic activities for the carbo-

nylation of organic compounds (vide infra). [Pt(dfepe)-(CO)(SO_3F)]$^+$ (dfepe = $(C_2F_5)_2PCH_2CH_2P(C_2F_5)_2$), [Pt(dfepe)(CO)($CF_3SO_3$)]$^+$, [Pt(dfepe)(CO)($CH_3$)]$^+$ and [Pt(dfepe)$(CO)_2$]$^{2+}$ are observed in FSO_3H and CF_3SO_3H solutions, respectively [102].

It was known that a number of copper(I) compounds absorb carbon monoxide with the CO/Cu stoichiometric ratio ≤ 1.0 to form Cu(CO)X under various conditions [128–134]. Souma et al. previously reported the formation of $Cu(CO)_4^+$, $Cu(CO)_3^+$ and $Cu(CO)^+$ from Cu_2O, which are in equilibrium in strong acids such as H_2SO_4, CF_3SO_3H, HSO_3F, HF and $BF_3 \cdot H_2O$, while $Cu(CO)_2^+$ was not considered [103]. Recent re-examination [127] of this system shows that Cu_2O or Cu reacts with CO in the above protic acids to form the solvated cations of $Cu(CO)_n^+$ ($n = 1$–4), which are in equilibrium in the strong acids. The IR and Raman spectra show that $Cu(CO)_2^+$ is bent (C_{2v}) and $Cu(CO)_3^+$ is non-planar (C_{3v}), and therefore, Cu^+ seems to assume a tetrahedral coordination geometry, in which the coordination sites unoccupied by CO ligands are occupied by the solvent molecules, in contrast to the formation of the two-coordinate, linear structure ($D_{\infty h}$) for [$Cu(CO)_2$]$^+$ and the three-coordinate, trigonal-planar structure (D_{3h}) for [

Table 2
Infrared C–O stretching frequencies ν(CO) for homoleptic metal carbonyl cations and related species in rare-gas matrices

Cation [a]	ν(CO) [b] (cm^{-1})	References
$ScCO^+$	1962.4 (1949.9)	[161]
$Sc(CO)_2^+$	1926.0 (1922.6)	[161]
$Sc(CO)_3^+$	1974.20	[161]
$TiCO^+$	2041.3	[162]
VCO^+ [c]	2116.3	[162]
$CrCO^+$	2200.8	[73]
$MoCO^+$	2189.1	[73]
$MnCO^+$	2089.5	[163]
$ReCO^+$	2102.1	[163]
$FeCO^+$	2123.0	[164,165]
$Fe(CO)_2^+$	2134.0	[164,165]
$RuCO^+$	2134.9	[166]
$OsCO^+$	2106.0	[166]
$CoCO^+$	2165.5	[167]
$Co(CO)_2^+$	2168.9	[167]
$RhCO^+$	2174.1	[167,168]
$Rh(CO)_2^+$	2184.7	[167,168]
$Rh(CO)_3^+$	2167.8	[167,168]
$Rh(CO)_4^+$	2161.5	[167]
$IrCO^+$	2156.5	[167]
$Ir(CO)_2^+$	2153.8	[167]
$NiCO^+$	2206.5	[169]
$Ni(CO)_2^+$	2205.3 (2209.2)	[169]
$Ni(CO)_3^+$	2192.4, 2186.2	[169]
$Ni(CO)_4^+$	2176.2	[169]
$PdCO^+$	2206.4	[169]
$Pd(CO)_2^+$	2210.5	[169]
$PtCO^+$	2204.7	[169]
$Pt(CO)_2^+$	2210.3	[169]
$Pt(CO)_3^+$	2207.9	[169]
$CuCO^+$	2234.4	[135]
$CuCO^+$ [c]	2174.4	[135]
$Cu(CO)_2^+$	2230.4 (2233.1)	[135]
$Cu(CO)_3^+$	2211.3	[135]
$Cu(CO)_4^+$	2202.1	[135]
$AgCO^+$	2233.1	[170]
$Ag(CO)_2^+$	2234.6	[170]
$Ag(CO)_3^+$	2216.0	[170]
$Ag(CO)_4^+$	2205.7	[170]
$AuCO^+$	2236.8 (2238.9)	[170]
$Au(CO)_2^+$	2233.4	[170]
$Au(CO)_3^+$	2203.5	[170]
$Au(CO)_4^+$	2193.5	[170]
$Sc(CO)O^+$ [c]	2221.8 (2207.2)	[171]
$Y(CO)O^+$ [c]	2206.0 (2203.3)	[171]
$U(CO)O^+$	2073.0	[172]
$Th(CO)O^+$	2009.9	[172]
$Ti(CO)O^+$ [c]	2188.0 (2185.5)	[173]
$V(CO)O^+$ [c]	2205.4 (2203.3)	[173]
$Cr(CO)O^+$ [c]	2175.5	[174]
$Mn(CO)O^+$ [c]	2173.0 (2177.7)	[174]
CO^+	2194.3	[135]
$(CO)_2^+$	2056.3	[135]
CO	2140.8	[135]
CO [c]	2138.2	[135]

[a] In a neon matrix unless otherwise noted.
[b] Value in parenthesis for the species at a different site.
[c] In an argon matrix.

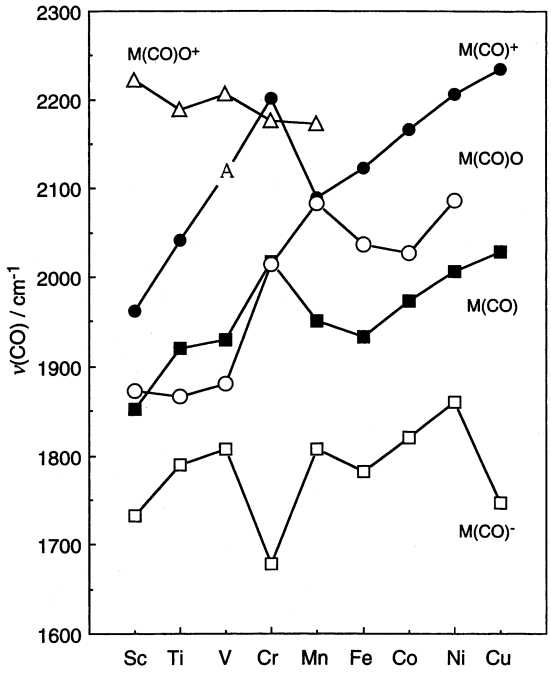

Fig. 1. Infrared C–O stretching frequencies ν(CO) for $M(CO)^+$, $M(CO)O^+$, M(CO)O, M(CO) and $M(CO)^-$ of the first-row transition metals in solid neon matrices (A denotes the argon matrix value) (Ref. [73]).

Table 3
Selected infrared C–O stretching frequencies ν(CO) for CO species of metal halides and oxides in argon matrices

Species	ν(CO) [a] (cm^{-1})	References
Li(CO)F	2185.1	[176]
Na(CO)F	2172.4	[176]
$Mg(CO)F_2$	2205	[176]
$Ca(CO)F_2$	2187.3, 2180.4	[176]
$Sr(CO)F_2$	2181.2, 2173.8, 2166.4	[176]
$Ba(CO)F_2$	2172.8, 2163.5, 2159.6	[176]
$Sc(CO)F_3$	2212.4, 2208.3	[176]
$Y(CO)F_3$	2197.5	[176]
$La(CO)F_3$	2185.2	[176]
$Nd(CO)F_3$	2187.4	[176]
$Gd(CO)F_3$	2194.4	[176]
$Ho(CO)F_3$	2198.2	[176]
$Lu(CO)F_3$	2204.8	[176]
$U(CO)F_4$	2181.8	[177]
$Cr(CO)F_2$	2188.4	[178]
$Mn(CO)F_2$	2183.2	[178]
$Ni(CO)F_2$	2200.4	[178]
$Ni(CO)Cl_2$	2189.2	[178]
cis-$Pt(CO)_2Cl_2$	2171.1, 2126.9	[39]
$Cu(CO)F_2$	2210.4	[178]
Cu(CO)Cl	2156.5	[179]
$Zn(CO)F_2$	2185.9	[178]
$Sn(CO)Cl_2$	2175.5	[146]
$Pb(CO)F_2$	2176.4	[146]
$Pb(CO)Cl_2$	2174.5	[146]
$Pb(CO)Br_2$	2161.2	[146]
$Pb(CO)I_2$	2149	[146]
Be(CO)O	2189.5	[180]
Sc(CO)O	1873.4	[171]
Y(CO)O	1861.5	[171]
$U(CO)O_2$ [b]	2021.6	[172]
U(CO)O [b]	1806.9	[172]
Th(CO)O [b]	1778.4, (1762.8) (1756.8)	[172]
Ti(CO)O	1866.8 (1864.4)	[173]
$Ti(CO)_2O$	2027.3, 1833.2	[173]
$V(CO)_2O_2$	2150.6, 2115.4 (2121.9) (2111.9)	[173]
V(CO)O	1881.1 (1874.3)	[173]
$V(CO)_2O$	1851.6	[173]
Cr(CO)O	2014.4	[174]
$Mn(CO)O_2$	2097.3	[174]
$Mn(CO)_2O_2$	2126.0, 2056.0	[174]
Mn(CO)O	2082.5	[163,174]
$Fe(CO)O_2$	2108.2	[174]
Fe(CO)O	2037.1	[174]
Co(CO)O	2026.6 (2018.8) (2015.3)	[174]
Ni(CO)O	2086.6 (2072.7)	[174]

[a] Value in parenthesis for the species at a different site.
[b] In a neon matrix.

Table 4
Selected infrared C–O stretching frequencies ν(CO) of M–CO species adsorbed on surfaces of metal oxides and halides

Surface	Conditions	ν(CO) (cm^{-1})	References
LiF	77 K; 100 face, low coverage	2155	[181]
NaCl	77 K; 100 face, low coverage	2159	[181]
NaI	77 K; 100 face, low coverage	2160	[181]
KCl	77 K; 100 face, low coverage	2153	[181]
CuF		2146	[182]
BeO	77 K; low coverage	2207, 2200, 2188	[145]
MgO	77K; 001 face, low coverage	2203, 2170, 2157	[183]
MgO	77 K; 100 face, low coverage	2170, 2151	[181]
CaO/Al_2O_3	300 K; 3% CaO	2182	[184]
La_2O_3	77 K	2175	[185,186]
CeO_2		~2170	[187]
TiO_2 (rutile)		2182	[187]
TiO_2 (anatase)	77 K; low coverage	2212, 2195, 2180	[145]
TiO_2/SiO_2	80 K; 7% TiO_2	2183–2178	[188]
ZrO_2		~2190	[189]
SO_4/ZrO_2		2220–2170	[189]
ZrO_2 [a]	273 K	2216	[127]
α-Cr_2O_3	77–298 K	2200–2162	[187,190]
Fe_2O_3	77 K	2165	[183]
CoO		2179	[182]
NiO	77K; 100 face, low coverage	2152	[181]
CuO/SiO_2	298 K	2136	[191]
ZnO	298 K	2212, 2200, 2187	[191]
ZnO	77 K; low coverage	2192, 2189	[145]
α-Al_2O_3	77 K; low coverage	2165, 2153	[192]
δ-Al_2O_3	77 K	2230–2184	[193]
η-Al_2O_3	77 K; low coverage	2235, 2202	[145]
SiO_2	77 K; low coverage	2158	[145]

[a] Surface of the zirconia ATR sensor of ReactIR spectrometer (ASi), washed with magic acid.

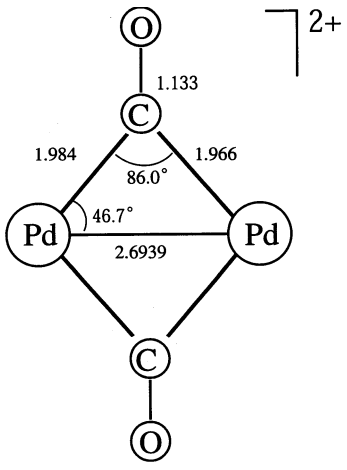

Fig. 2. Molecular structure of the [*cyclo*-$Pd_2(\mu\text{-}CO)_2]^{2+}$ cation (Ref. [100]). The bond lengths are in Å.

Table 5
Metal–metal Raman frequencies ν(M–M) of seletced metal carbonyl clusters

Compound	ν(M–M) (cm^{-1})	References
$[\{Hg(CO)\}_2][Sb_2F_{11}]_2$ [a]	169	[109,110]
$[\{Pt(CO)_3\}_2]^{2+}$ [b]	165	[69,70]
$(n\text{-}Pr_4N)_2[\{PtCl_2(CO)\}_2]$ [a]	170	[240]
$(n\text{-}Pr_4N)_2[\{PtBr_2(CO)\}_2]$ [a]	135	[240]
$[Ir_4(CO)_{12}H_2]^{2+}$ [b]	199, 163	[68]
$Ir_4(CO)_{12}$ [a]	207, 161, 131	[241]
$Os_3(CO)_{12}$ [a]	158, 117	[242]
$Ru_3(CO)_{12}$ [a]	185, 149	[242]
$Fe_2(CO)_9$ [a]	225	[243]
$Fe_3(CO)_{12}$ [a]	219	[243]
$(t\text{-}BuC_2\text{-}t\text{-}Bu)_2[\{Fe(CO)_2\}_2]$ [c]	284	[244]
$Re_2(CO)_{10}$ [a]	122	[245–248]
$Tc_2(CO)_{10}$ [d]	148	[245,246]
$Mn_2(CO)_{10}$ [a]	160	[245–247]
$(Et_4N)_2[\{W(CO)_5\}_2]$ [a]	111	[249]
$(Et_4N)_2[\{Mo(CO)_5\}_2]$ [a]	138	[249]
$[\{Cr(CO)_5\}_2]^{4+}$ [e]	334	[127]
$(Et_4N)_2[\{Cr(CO)_5\}_2]$ [a]	160	[249]

[a] In solid state.
[b] In concentrated H_2SO_4.
[c] In CS_2 solution.
[d] In cyclohexane.
[e] Tentative formulation for the species formed in magic acid, $HSO_3F \cdot SbF_5$ (1:1).

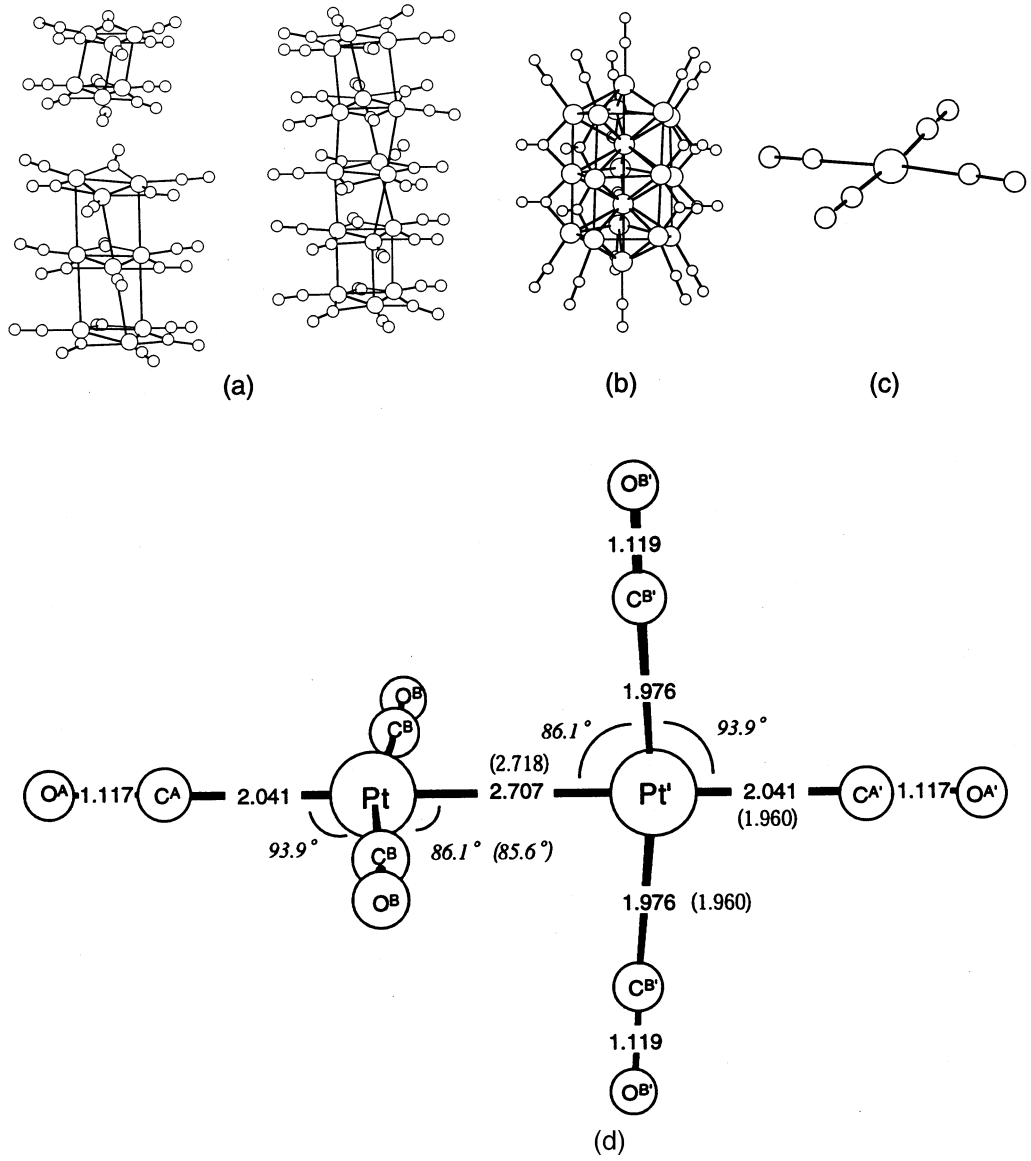

Fig. 3. The homoleptic platinum carbonyl complexes of (a) $[Pt_3(CO)_6]_n^{2-}$ ($n = 2$, 3, 5) (Ref. [253]), (b) $[Pt_{19}(CO)_{12}(\mu_2\text{-}CO)_{10}]^{4-}$ (Ref. [255]), (c) $[Pt(CO)_4]^{2+}$ (Ref. [77]) and (d) $[\{Pt(CO)_3\}_2]^{2+}$ (Ref. [70]). In the salt $[Pt(CO)_4][Sb_2F_{11}]_2$, there exist interionic interactions almost exclusively of the C--F type, which contribute to tight packing of the $[Pt(CO)_4]^{2+}$ cations and $[Sb_2F_{11}]^-$ anions as well as to the formation of extended structures (see Ref. [77]). For $[\{Pt(CO)_3\}_2]^{2+}$, the geometry optimization using B3LYP/cc-pVTZ predicts that the dihedral angle between the two coordination planes of the T-shaped $Pt(CO)_3$- groups is exactly 90.0° and the overall symmetry is D_{2d} (Ref. [70]). The platinum L_{III}-edge EXAFS data are shown in parentheses. The bond lengths are in Å.

Table 6
Spectroscopic data of metal hydridocarbonyl cations

Complex [a]	$\nu(CO)_{av}$ [b] (cm^{-1})	$\delta(^1H)$ (ppm)	$\delta(^{13}C)$ (ppm)	References
$[Fe(CO)_5H]^+$ [c]	2137 [d]	−8.1 [e]		[48,281]
$[Ru(CO)_5H]^+$		−7.2	180.5, 178.2	[282]
$[Ru_3(CO)_{12}H]^+$	2106 [f]	−19.4	201.8, 194.5, 184.9, 184.1, 179.1 [g]	[283–285]
$[Os(CO)_5H]^+$	2080	−8.2	159.0 [g]	[285,286]
$[Os_3(CO)_{12}H]^+$	2085	−19.9	177.6, 171.1, 166.7, 161.4, 160.8	[283–287]
$[Ir_4(CO)_{12}H_2]^{2+}$	2138	−19.6	144.2, 142.0	[68,285]

[a] In concentrated H_2SO_4 unless otherwise stated.
[b] Average of $\nu(CO)_{IR}$.
[c] Decomposes rapidly in concentrated H_2SO_4.
[d] As $[PF_6]^-$ salt.
[e] In $BF_3 \cdot H_2O$–CF_3COOH.
[f] In CF_3COOH.
[g] In HF solution.

Table 7
Metal carbonyl cation-catalyzed carbonylation of olefins and alcohols in concentrated H_2SO_4 at 1 atm of CO

Substrate	Carbonyl catalyst	Tertiary carboxylic acid	Yield [a] (%)	References
1-Pentene	Pt(I) [b]	2,2-Dimethylbutanoic	70	[71]
		Others	1	
1-Hexene	Pd(I) [c]	2,2-Dimethylpentanoic	48	[66]
		2-Methyl-2-ethylbutanoic	23	
		Others	1	
1-Octene	Rh(I) [d]	2,2-Dimethylheptanoic	41	[67]
		2-Methyl-2-ethylhexanoic	22	
		2-Methyl-2-propylpentanoic	10	
		Others	3	
1-Decene	Au(I) [e]	2,2-Dimethylnonanoic	33	[65]
		2-Methyl-2-ethyloctanoic	16	
		2-Methyl-2-propylheptanoic	12	
		2-Methyl-2-butylhexanoic	5	
		Others	4	
Cyclohexene	Cu(I) [f]	1-Methylcyclopentanecarboxylic	63	[294]
t-Butanol	Pd(I) [c]	2,2-Dimethylpropanoic	70	[66]
		Others	2	
1-Hexanol	Ag(I) [g]	2,2-Dimethylpentanoic	79	[296]
		2-Methy-2-ethylbutanoic	19	
1-Octanol	Cu(I) [h]	2,2-Dimethylheptanoic	72	[297]
		2-Methyl-2-ethylhexanoic	15	
		2-Methyl-2-propylpentanoic	5	
Cyclohexanol	Ag(I) [g]	1-Methylcyclopentanecarboxylic	81	[296]

[a] Based on substrate.
[b] PtO_2/substrate = 2.0 mmol/5.0 mmol, 96% H_2SO_4 10 ml, 25 °C.
[c] $PdSO_4$/substrate = 1.0 mmol/5.0 mmol, 96% H_2SO_4 10 ml, 25 °C.
[d] $Rh_4(CO)_{12}$/substrate = 0.17 mmol/2.5 mmol, 96% H_2SO_4 5 ml, 25 °C.
[e] Au_2O_3/substrate = 0.5 mmol/5.0 mmol, 96% H_2SO_4 10 ml, 25 °C.
[f] Cu_2O/substrate = 20 mmol/200 mmol, 98% H_2SO_4 105 ml, 30 °C.
[g] Ag_2O/substrate = 8.0 mmol/20 mmol, 98% H_2SO_4 40 ml, 30 °C.
[h] Cu_2O/substrate = 4.0 mmol/20 mmol, 98% H_2SO_4 21 ml, 30 °C.

Table 8
Dependence on H_2SO_4 concentration of the ratio of CO/Au^+ and the yield of tertiary carboxylic acids from 1-hexene [a]

Concentration of H_2SO_4 (wt.%)	CO/Au^+	Yield of tertiary C_7 acids [b] (%)
75	1.00	0
80	1.05	20
85	1.10	32
90	1.36	58
93	1.58	79
96	1.65	80

[a] Au_2O_3/(1-hexene) = 0.5 mmol/5.0 mmol, H_2SO_4 10 ml, CO 1 atm, r.t. (Ref. [65]).
[b] Based on 1-hexene.

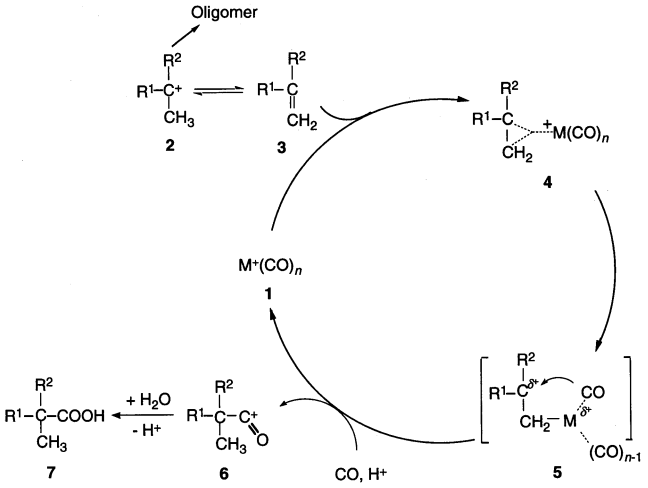
Oligomer
R2
R1–C+
CH3
2
R1–C
CH2
3
M+(CO)n
1
R1–C
+M(CO)n
CH2
4
R1–C
CO
CH2– M
(CO)n-1
5
R1–C–COOH
CH3
7
+ H2O
- H+
R1–C–C+
O
6
CO, H+

Scheme 1.

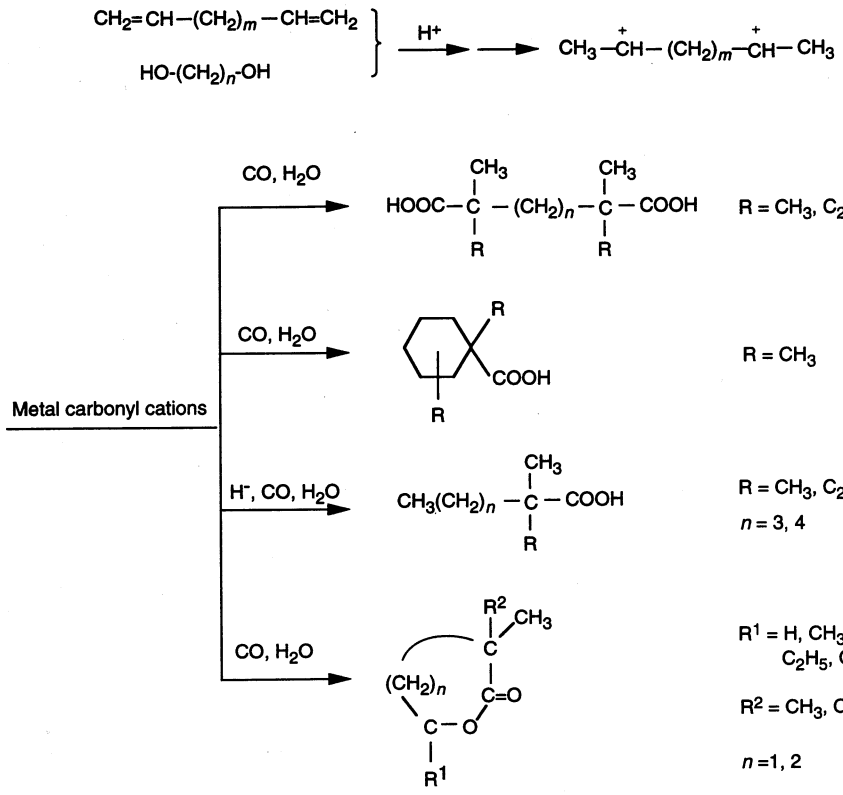

Scheme 2.

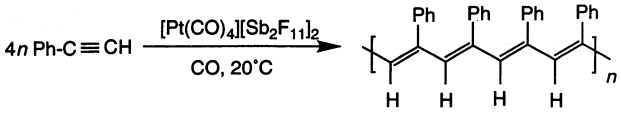

Table 9
Copper(I) carbonyl-catalyzed carbonylation of dienes, diols, aldehydes and saturated hydrocarbons in strong acids at 1 atm of CO

Substrate	Temperature (°C)	Product	Yield[a] %	References
1,5-Hexadiene [b]	0–5	2-Ethyl-4-pentanolide	46	[313]
1,7-Octadiene [b]	3–8	2,2-Dimethyl-4-heptanolide	15	[313]
		2,2-Dimethyl-5-heptanolide	8	
		2,2-Dimethylheptanoic acid	14	
		2-Methyl-2-ethylhexanoic acid	6	
		1,4-Dimethylcyclohexanecarboxylic acid	35	
1,9-Decadiene [b,c]	5–10	2-Methyl-2-ethyl-4-octanolide	20	[313]
		2-Methyl-2-ethyl-5-octanolide	15	
		2,2,7,7-Tetramethyloctanedioic acid	45	
		2-Ethyl-2,6,6-trimethylheptanedioic acid	10	
1,8-Octanediol [b]	20–25	2,2-Dimethyl-4-heptanolide	35	[313]
		2,2-Dimethyl-5-heptanolide	40	
1,12-Dodecanediol [b]	20	1,4- and 1,5-Lactone	50	[313]
		2,2,9,9-Tetramethyldecanedioic acid	38	
		2-Ethyl-2,8,8-trimethylnonanedioic acid	9	
Formaldehyde [d]	20	Glycolic acid	96	[315]
Octane [e]	−2 to 2	2,2-Dimethylpropanoic acid	195	[316]

[a] Based on substrate.
[b] Cu_2O/substrate = 8.0 mmol/30 mmol, 98% H_2SO_4 30 ml.
[c] 10 ml of HSO_3F added.
[d] Cu_2O/HCHO = 1.0 g/2.5 g, 98% H_2SO_4 20 ml.
[e] Cu_2O/octane = 6.0 mmol/30 mmol, HSO_3F 20 ml, SbF_5 10 ml.